Phase transition and winding properties of a flexible polymer adsorbed to a rigid perioidic copolymer

Lei Liu,[1] David Schubert,[1] Min Chu,[1] and Dieter W. Heermann[1,2,3]
[1]*Institute for Theoretical Physics, Heidelberg University, Heidelberg 69120, Germany*
[2]*The Jackson Laboratory, Bar Harbor, Maine 04609, USA*
[3]*Shanghai Institute of Biological Sciences, Chinese Academy of Sciences, Shanghai 200031, People's Republic of China*
(Received 2 May 2014; revised manuscript received 7 November 2014; published 11 March 2015)

Motivated by the noncovalent binding of polypeptides to DNA, the adsorption of a flexible polymer to a rigid periodic copolymer is studied in two dimensions and three dimensions. The fraction of adsorbed monomers, the specific heat, and the Binder cumulant are analyzed and compared with analytical results for an ideal chain. As the interaction strength ϵ increases, a second-order phase transition occurs from a nonadsorbed state to an adsorbed state, in two dimensions, and a higher-order transition occurs in three dimensions. The transition point is estimated as $\epsilon_0 \sim 2.2$ for $d = 2$ and $\epsilon_0 \sim 2.1$ for $d = 3$, where ϵ is given in units of k_BT. The dependence of the number of adsorbed monomers $N_{\rm ads}$ on the chain length L of the flexible polymer shows a power law scaling relation $N_{\rm ads} \sim L^{\phi}$, with $\phi \sim 0.46, 0.42$ for $d = 2,3$, respectively. We also find an optimal $\epsilon \sim 2.8$ for the winding of the flexible polymer around the rigid one in three dimensions. Compared to the adsorbed monomers, the successive nonadsorbed monomers contribute more to the winding. When the interaction is strong, $\epsilon > 3.5$, the winding value or the number of winding turns of the flexible polymer becomes linearly dependent on the chain length.

DOI: 10.1103/PhysRevE.91.032601 PACS number(s): 82.35.Lr

I. INTRODUCTION

Contrary to the traditional view that a functional protein usually possesses a stable three-dimensional structure, more and more functional intrinsically disordered protein domains of significant size are reported [1,2]. They interact with DNA, RNA, and other protein domains, and play several important roles in cells such as transcriptional regulation, translation, and cellular signal transduction [3,4]. Many intrinsically disordered proteins undergo a transition from a random-coil-like unbound state to a more ordered bound state of stable secondary or tertiary structure, i.e., a so-called folding while binding process [5,6]. For example, the binding of the multi-C_2H_2 zinc finger protein, which behaves like a wormlike chain [7], to its target DNA sites results in an orientational restraint of successive zinc fingers and facilitates the whole protein to wind around the DNA along its helical major groove [8]. It is well known that the giant loss of entropy of a protein from unbound to bound state should be compensated with the protein-DNA binding enthalpy gain [9,10].

Another macromolecular system of current interest is the polymer-carbon nanotube hybrid, which consists of a carbon nanotube (CNT) coated with a self-assembled monolayer of flexible or semiflexible polymer chains [11,12]. Several experiments confirmed that wrapping is a general phenomenon occurring between polymers and CNTs, and some polymers are reported to wrap CNTs in a distinct, helical-type conformation, like poly(sacchrides) [13], poly(dialkylsilanes) [14], and single-stranded DNA [15,16]. This noncovalent polymer wrapping can affect the properties of the CNTs, such as the solubility, dispersity, strength, toughness, and conductance, and hence enhances its functionality in numerous proposed applications [17–19].

There are studies on both intrinsically disordered protein DNA and polymer CNT, with either Monte Carlo or molecular dynamics methods on a coarse-grained or atomistic scale [20–22]. For example, Levy's group uncovered the asymmetric role of zinc fingers in the DNA-scanning process of the inducible transcription factor Egr-1 based on a Go-type model [23,24]. Tallury and Pasquinelli found that polymers with stiff and semiflexible backbones, but not those with flexible backbones, tend to wrap around the CNTs in a periodic helical way via atomistic molecular dynamics simulations [25,26]. However, all these studies focused on one or a few specific molecular systems, and it was not fully understood how the adsorptive interaction between the polypeptides and DNA, or the polymer and CNT, influences the binding and the winding.

To answer these questions, a generic polymer-polymer coarse-grained model was developed. The intrinsically disordered protein is modeled as a flexible polymer chain. Since the adsorbing sites for proteins along DNA usually are not consecutive, the DNA molecule is modeled as a rigid periodic copolymer. Conformation properties of the polymer-polymer complex were investigated with different adsorptive interaction and different chain lengths. The phase transition from a nonadsorbed state to an adsorbed state and the characteristics of the flexible polymer wrapping around the rigid one are analyzed. In Sec. II, we discuss the theoretical work on the adsorption of an ideal chain. In Sec. III, the model and the simulation method are briefly introduced. Then the results for the phase transition and winding are discussed in two different parts. Finally, we present a short summary of our main conclusions.

II. THEORY

Research interest on similar problems dates back to the 1960's. Rubin studied the adsorption of an ideal chain on a long rigid-rod molecule by the transfer-matrix method [27]. There the adsorbing rodlike molecule is represented by the lattice sites on the z axis of a cubic lattice. The adsorptive interaction strength is ϵ, and the adsorption energy per monomer is $-\epsilon$ in

units of k_BT. Given that the first monomer is grafted on the z axis and the length of the flexible chain approaching infinity, the average fraction of adsorbed monomers f_{ads} is found to be equal to zero below a transition point $\epsilon < \epsilon_0$. What is more, the kth derivative of f_{ads} at ϵ_0 equals zero for any $k \geqslant 1$, suggesting an infinite-order phase transition. Numeric results of f_{ads} and the specific heat $C = \langle (E - \langle E \rangle)^2 \rangle / Lk_BT^2$, where E is the energy of the system, are plotted in the insets of Figs. 2(a) and 2(b), respectively.

For the adsorption of an ideal chain to an impenetrable straight line in two dimensions, one can directly apply the solution of the adsorption of an ideal chain to an impenetrable flat surface [28]. Consider a lattice model of the chain-surface system in which the adsorbing surface corresponds to the x-y plane and the chain is represented by a random walk in half of the space $z > 0$. Each lattice site is surrounded by Z nearest-neighbor sites, while Z_0 of them of the same z value are called to locate in the same layer. At any moment, the walker can only move to one of the current nearest-neighbor sites in the next step. For a random walker who starts on the adsorbing surface, the probability that at the Nth step the random walker is located in the kth lattice layer is $P_k(N)$. The key recurrence equation for adsorption on a plane is

$$P_k(N) = \tfrac{1}{2}aP_{k+1}(N-1) + (1-a)P_k(N-1) + \tfrac{1}{2}aP_{k-1}(N-1) \quad (1)$$

for $k \geqslant 1$, where $a = (Z - Z_0)/Z$. This describes that if at the Nth step the random walker is in the kth layer he must be in the $k-1$, k, or $(k+1)$th layer at the $(N-1)$th step. On the adsorbing surface where $k = 0$, we have the boundary condition

$$P_0(N) = \tfrac{1}{2}ae^{\epsilon}P_1(N-1) + (1-a)e^{\epsilon}P_0(N-1), \quad (2)$$

where the factor e^{ϵ} accounts for a greater probability of a step lying on the adsorbing surface. It is reported [28] that this system undergoes a second-order phase transition as the chain length $L \to \infty$. Again the chain is nonadsorbed ($f_{\text{ads}} = 0$) below ϵ_0, but the specific heat C jumps discontinuously from zero to a finite peak at ϵ_0. The insets in Figs. 2(c) and 2(d) give the corresponding numeric solution of f_{ads} and C as a function of ϵ.

Concerning the problem of the adsorption of an ideal chain on an axis in two dimensions, $P_k(N)$ can be also regarded as the probability that a random walker, in a half $x - y$ plane ($y > 0$), is located in the kth lattice layer ($y = k$) at the Nth step, when he starts from the attracting x axis. Then in a two-dimensional simple square lattice, one simply sets $a = (4-2)/4 = 0.5$ and it should have the same phase transition behavior as above.

A more general scaling analysis for the adsorption of flexible chain onto any object S [29] shows that $f_{\text{ads}} = 0$ for $\epsilon < \epsilon_0$ and $f_{\text{ads}} > 0$ for $\epsilon > \epsilon_0$ when the chain length $L \to \infty$. Close to ϵ_0, the number of adsorbed monomer N_{ads} follows the relation [30]

$$N_{\text{ads}} = L^{\phi}F[(\epsilon - \epsilon_0)L^{\nu}], \quad (3)$$

where $F(x)$ is a scaling function. The relation between the crossover exponent ϕ and the critical exponent ν has been studied. Regarding the adsorption of a polymer on a surface in three dimensions, a lattice simulation by Eisenriegler, Kremer, and Binder reports that $\phi \simeq 0.59 \simeq \nu_{3D}$ [31], which is also obtained by Descas *et al.* [32]. Using a different algorithm, Hegger and Grassberger find $\phi \sim 0.5$ [33], and this result is supported by other simulations [34]. If the surface is penetrable and neutral (with $\epsilon_0 = 0$), ϕ is related to ν via $\phi = 1 - \nu$ [35]. Bhattacharya *et al.* found that the value of ϕ depends essentially on the degree of interaction between different loops in a polymer, and varies in the range of $0.34 \leqslant \phi \leqslant 0.59$ [36].

III. MODEL AND SIMULATION

In our model, both in two dimensions and three dimensions, the rigid molecule (e.g., DNA) is represented by an infinitely long copolymer with periodically distributed adsorption sites on it (see Fig. 1). The flexible molecule (polypeptides) is modeled as a flexible polymer of length L. We implement this using the bond fluctuation model [37] for the cubic lattice, where the bond lengths of the flexible polymer can vary from 2 to $\sqrt{10}$. The rigid polymer lies on the x axis. Since the closest integer to the *a priori* mean bond length of a polymer in the bond fluctuation model is 3, the distance between the adsorbing sites is chosen to be 3. Because of the excluded volume, one adsorption site cannot be occupied by two monomers simultaneously, and the distance from the monomer of the flexible polymer to the rigid one is $s \geqslant 2$. One monomer of the flexible polymer is considered to locate on the surface of the rigid molecule if $s = 2$ in two dimensions, or $2 \leqslant s \leqslant \sqrt{8}$ in three dimensions, but it is adsorbed *only* when it resides on the surface of an adsorbing site, i.e., it has the same x coordinate value as an adsorbing site.

The simulations were performed using the standard Metropolis algorithm [38], where an adsorbed monomer can only leave the adsorption site with a probability $\exp(-\epsilon/k_BT)$. It is guaranteed that at least one monomer of the flexible polymer, not adsorbed necessarily, is on the surface of the rigid copolymer. For different $L \in \{10,20,40,80,160,200\}$ and $\epsilon \in$

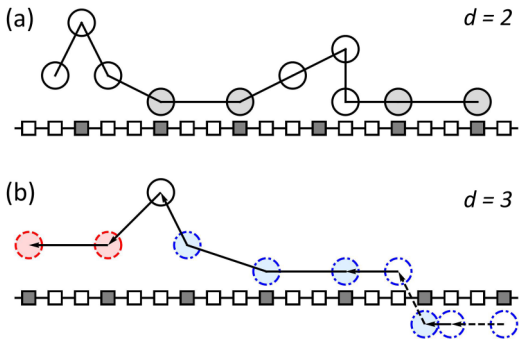

FIG. 1. (Color online) An illustration of our model in two dimensions (a) and in three dimensions (b). The z axis is perpendicular to and points out of the plane. Monomers of the rigid polymer are represented by squares, where the adsorbing sites are colored gray. Monomers of the flexible polymer are represented by circles of solid black edges ($z = 0$), dashed red edges ($z > 0$), and dash-dotted blue edges ($z < 0$). Circles representing adsorbed monomers are filled. In (b), bonds from monomer i to $i+1$ are drawn using solid lines (parallel to the plane), solid arrows (going out of the plane), and dashed arrows (going into the plane).

[0.0,5.0] with a step 0.1, we first calculated the sampling interval Δ_t from the autocorrelation time of the radius of gyration R_g of the flexible polymer (e.g., $\Delta_t \sim 10^7$ Monte Carlo steps for $L = 200$, $\epsilon = 3.0$). Then after equilibration, 10^4 independent conformations with interval Δ_t were sampled for each pair of parameters $\{L,\epsilon\}$ to calculate the ensemble averaged properties of interest.

Since the first monomer of the flexible chain is always fixed and adsorbed in the theoretical work, we also calculated the adsorption with the first monomer grafted.

IV. RESULTS

A. Phase transition

The dependence of the fraction of adsorbed monomers $f_{\rm ads}$ and the specific heat C on the adsorptive interaction strength ϵ for various chain lengths are presented in Fig. 2. In both dimensions, due to the finite size effect, the transition gets sharper when L increases. For longer polymers, the $f_{\rm ads}$ is almost zero for small ϵ. It is apparent that there is a steeper rise within the transition region in two dimensions than in three dimensions. Also a higher fraction of the flexible polymer is adsorbed in two dimensions than in three dimensions when the interaction is strong (e.g., $\epsilon = 5.0$). Concerning the specific heat, for $L = 200$, C roughly jumps vertically to a higher peak in two dimensions, while it climbs up to a lower maximum with a flatter slope in three dimensions. All of these features appear in the theoretical results for an ideal chain too. Therefore we expect a second-order phase transition for $d = 2$, and a higher-order (larger than 2) transition for $d = 3$. In addition, as the flexible polymer becomes longer and longer, the peak height of the specific heat increases monotonically in two dimensions, and it starts increasing followed by a decline in three dimensions. However, it converges in either case. Taking the number of adsorbed monomers $N_{\rm ads}$ as an order parameter, the dependence of susceptibility $\chi = \langle N_{\rm ads}^2\rangle - \langle N_{\rm ads}\rangle^2$ on ϵ as $L \to \infty$ (data not shown here) also supports the conclusion drawn from the specific heat.

In order to determine the transition point ϵ_0, we perform the analysis of the Binder cumulant $U = 1 - \langle N_{\rm ads}^2\rangle/3\langle N_{\rm ads}\rangle^2$ [30,38]. It is known that, providing the chain length $L \to \infty$, U approaches 2/3 for $\epsilon > \epsilon_0$, and it tends to a nonzero value at ϵ_0 independent of L. Hence, for pairs of different finite chain lengths $\{L,L'\}$, the ratio between the Binder cumulants $U_L/U_{L'}$ should equal to 1 near the transition point. Figures 3(a) and 3(c) show U as a function of L^{-1} around ϵ_0 for $d = 2,3$, respectively. U shows different behavior for $\epsilon > \epsilon_0$ and $\epsilon < \epsilon_0$ in both dimensions. This suggests that $\epsilon_0 \sim 2.3$ in two dimensions and $\epsilon_0 \sim 2.1$ in three dimensions. The ratios of the Binder cumulants for different pairs of chain lengths versus the interaction strength are plotted in Figs. 3(b) and 3(d). According to the points, which cross over the horizontal line $U_L/U_{L'} = 1$, we found $2.25 < \epsilon_0 < 2.35$ and $2.05 < \epsilon_0 < 2.15$, for $d = 2$ and 3, respectively, but this only gives us a rough range of the transition point.

Since it is reported [30,32,34] that the ratio between the perpendicular and parallel components of the mean square radius of gyration $\langle R_{g\perp}^2\rangle/\langle R_{g\parallel}^2\rangle$ should be independent of the

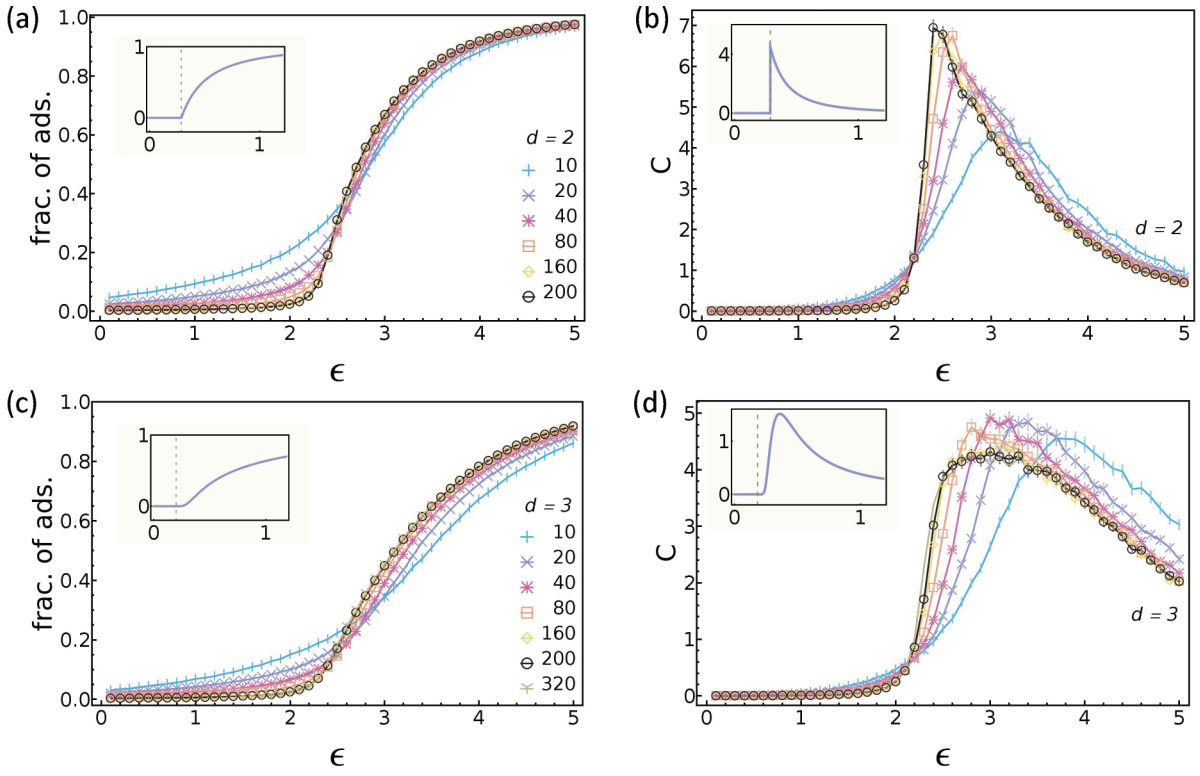

FIG. 2. (Color online) Fraction of adsorbed monomers (a, c) and specific heat (b, d) for different chain lengths $L \in \{10,20,40,80,160,200,320\}$ and different adsorptive interaction strength ϵ in dimension $d = 2,3$. Subplot (b, d) has the same legend as (a, c), respectively. The corresponding theoretical results for an ideal chain in two dimensions [28] and in three dimensions [27] are shown in the insets, while the vertical dashed lines indicate the location of the transition point ϵ_0.

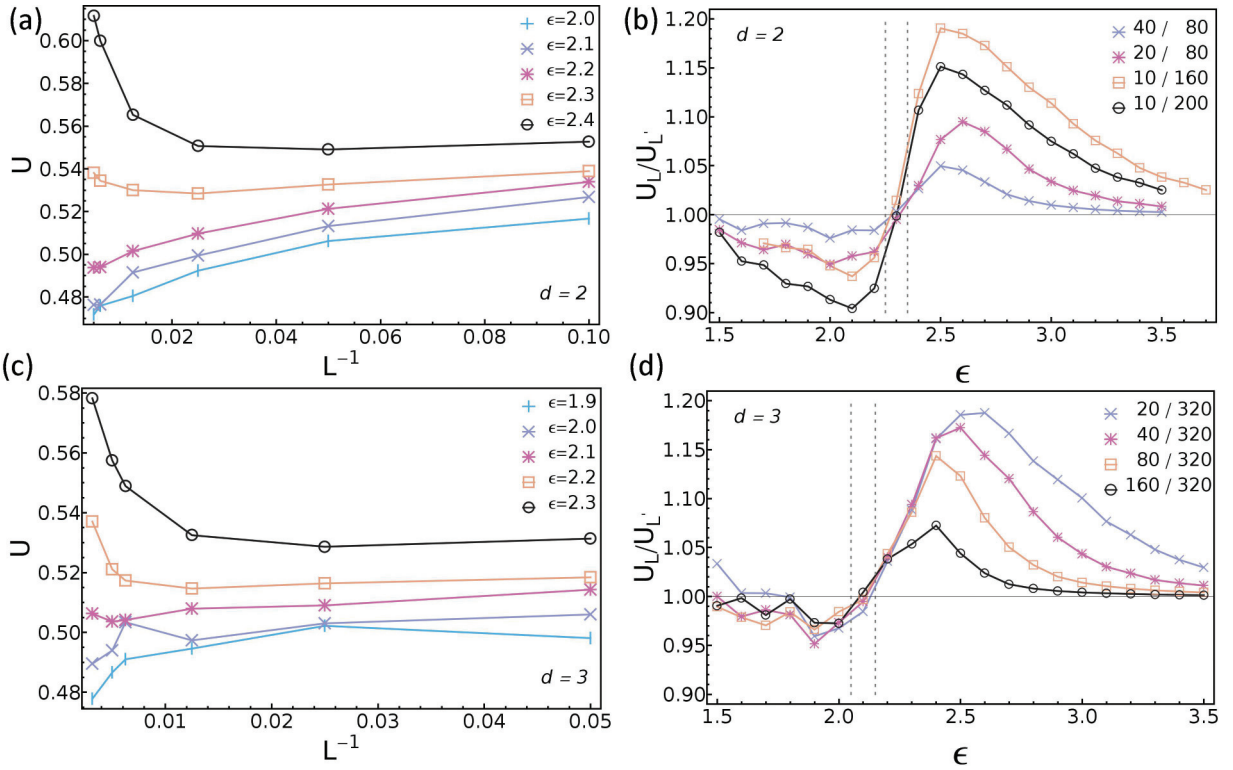

FIG. 3. (Color online) Binder cumulant U vs the inverse of chain length L^{-1} around ϵ_0 (a, c), and the ratio between U of different pairs of chain lengths $\{L/L'\} \in \{20/320,40/320,80/320,160/320\}$ vs the adsorptive interaction strength ϵ (b, d) in $d = 2,3$. The intersection points are located within the pair of vertical dashed lines in (b, d).

chain length L at the transition point in the surface adsorption problem, the dependence of this ratio on the interaction strength for different chain lengths is presented in Fig. 4. In two dimensions, the curves for different L intersect at $\epsilon_0 = 2.2$, but in three dimensions they collapse onto each other at low adsorptive interaction and do not intersect at one clear point. The difference can be explained if one notices that the flexible polymer can wrap around the rigid polymer in three dimensions, but not in two dimensions (due to the dimensionality of the space and the excluded volume interaction between the flexible polymer and the rigid one). Swelling perpendicularly at small ϵ leads to a larger $Rg_\perp$. Because of the same reason, $\langle R_{g\perp}^2\rangle/\langle R_{g\parallel}^2\rangle \sim 1$ for $d = 2$, but $\langle R_{g\perp}^2\rangle/\langle R_{g\parallel}^2\rangle > 2$ for $d = 3$, for weak adsorptive interaction.

We have also measured the dependence of the number of adsorbed monomers $N_{\rm ads}$ on L in the transition region [see Figs. 5(a) and 5(c) for $d = 2,3$, respectively]. In agreement with the scaling analysis, a linear curve in the log-log plot indicates a power law relation $N_{\rm ads} \sim L^{\phi}$ for both dimensions. The exponent values of $\{\phi,\nu\}$ are further calculated by fitting the scaling

$$N_{\rm ads}L^{-\phi} = a_0 + a_1(\epsilon - \epsilon_0)L^{\nu} + O[(\epsilon - \epsilon_0)^2 L^{\nu}], \quad (4)$$

following the method from Luo [30]. In brief, taking two dimensions as an example, $N_{\rm ads}$ at $\epsilon \in [2.0,2.4]$ with a step of 0.01 are obtained from quadratic interpolation from the simulation data at $\epsilon \in \{2.0,2.1,2.2,2.3,2.4\}$. Then, $\{\epsilon_0,\phi\}$ are determined by a best fit to a power law. ν is the value which minimizes the deviation from the relation $N_{\rm ads}L^{\phi} \sim (\epsilon - \epsilon_0)L^{\nu}$ of the simulation data to a parabolic function.

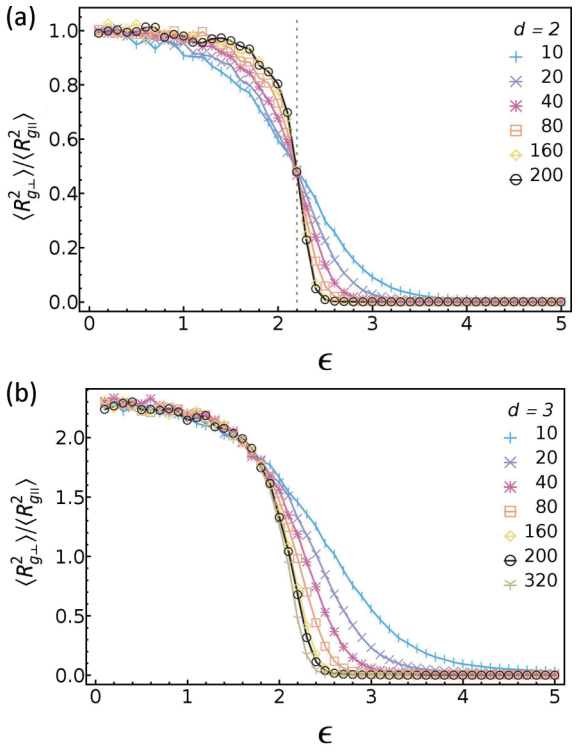

FIG. 4. (Color online) The ratio between the perpendicular and parallel components of the mean square radius of gyration $\langle R_{g\perp}^2\rangle/\langle R_{g\parallel}^2\rangle$ vs ϵ in two dimensions (a) and three dimensions (b). The vertical dashed line in (a) indicates the location of the intersection point.

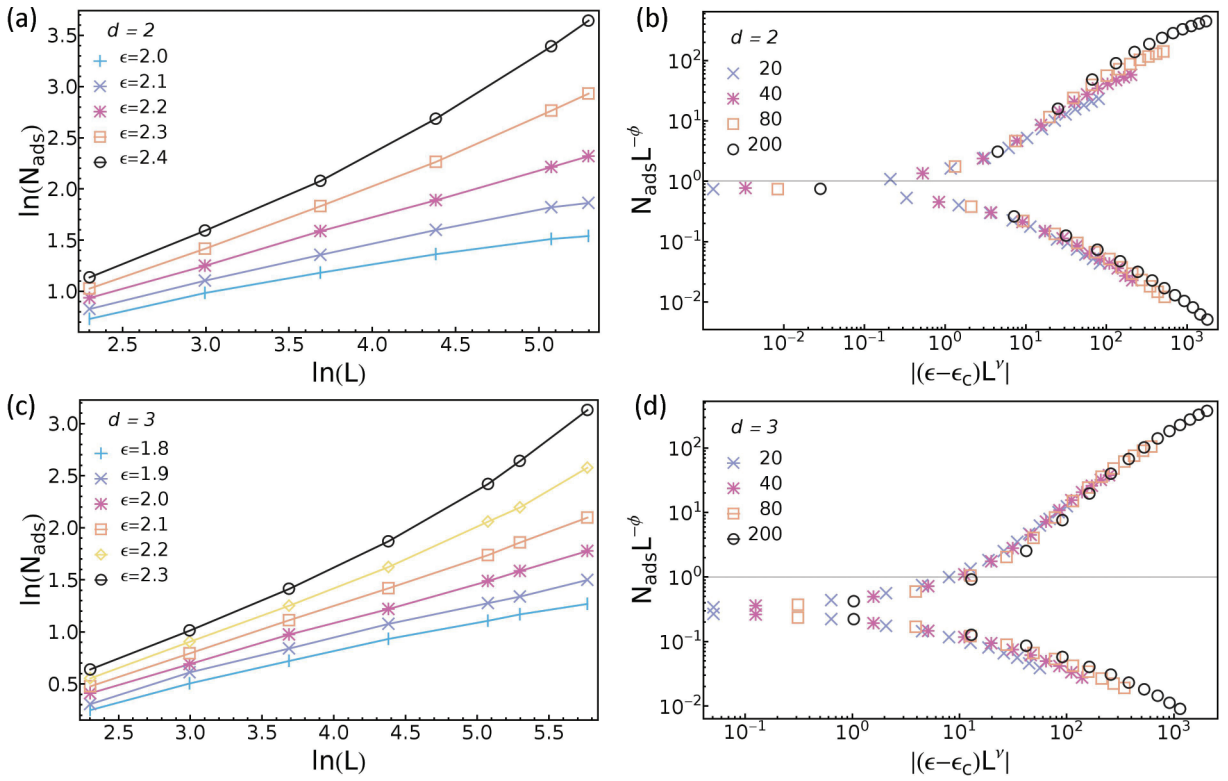

FIG. 5. (Color online) Log-log plot of the number of adsorbed monomers N_{ads} vs the chain length L around ϵ_0 (a, c), and the scaling of N_{ads} with $\{\epsilon,\phi,\nu\}$ equals $\{2.20,0.46,0.58\}$ in two dimensions (b) and $\{2.05,0.42,0.57\}$ in three dimensions (d) for various chain lengths.

Figures 5(b) and 5(d) show the scaled N_{ads} with $\epsilon_0 = 2.20$, $\phi = 0.46$, $\nu = 0.58$ for $d = 2$, and $\epsilon_0 = 2.05$, $\phi = 0.42$, $\nu = 0.57$ for $d = 3$. We can see that all data collapse quite well even for ϵ far from ϵ_0. It is quite interesting to find that our fitted values satisfy $\phi \sim 1 - \nu$, which was proposed by De Gennes [35].

Finally in Figs. 6(a) and 6(c) we compare f_{ads} for the chain having the first monomer always grafted to the rigid polymer with that for the nongrafted polymer used in our model. When the polymer is short, the grafted polymer always has a higher fraction of adsorption than the nongrafted one, but the difference between them diminishes as the polymer gets longer. Hence the above discussion about the phase transition should also apply to the grafted polymer, providing L approaches infinity. However, deviations can be found if one looks at the perpendicular monomer density $\rho_\perp$ profile for the grafted and nongrafted polymer in Figs. 6(b) and 6(d). At low adsorptive interaction, compared to the nongrafted polymer, the grafted one is expelled further away from the rigid polymer. At high interaction, since most of the polymer is adsorbed on the surface, this difference disappears.

B. Winding properties

Another property of special interest is how the flexible polymer winds or wraps around the rigid one in three dimensions. The winding value w is defined as a function of the contour length l of the flexible polymer, for $l \in \{1,2,\ldots,L\}$. We have

$$w(i+1) = w(i) + d\varphi, \tag{5}$$

while the flexible polymer rotates around the rigid one from monomer i to $i+1$ by an angle $d\varphi$ (see Fig. 7). One turn is counted if $|\Delta_w| = |w_e - w_s|$ exceeds 2π, where w_s and w_e are the winding values at the head and tail of a segment of the flexible polymer, respectively. Looking along the rigid molecule, the flexible polymer can wind either clockwise

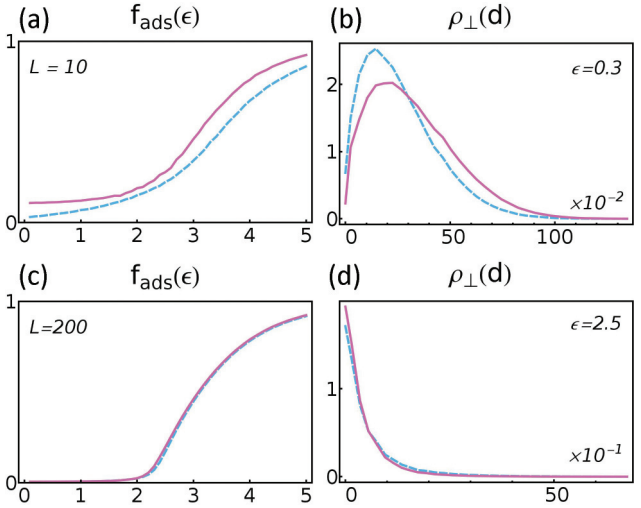

FIG. 6. (Color online) Fraction of adsorbed monomers for nongrafted (dashed blue line) and grafted polymer (solid purple line) with $L = 10,200$ in (a, c), respectively, and the perpendicular monomer density $\rho_\perp$ vs the distance from the monomer to the rigid polymer surface for nongrafted (dashed blue line) and grafted polymer (solid purple line) with $L = 200$ and $\epsilon = 0.3,2.5$ in (b, d), respectively.

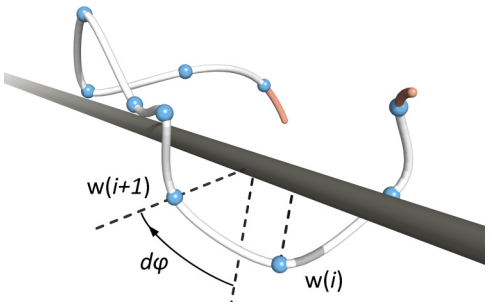

FIG. 7. (Color online) Winding and turn. The winding value w, as a function of the contour length l along the flexible polymer, varies from $w(i)$ to $w(i+1)$ with $d\varphi$, by which the flexible polymer rotates around the rigid one from monomer i to $i+1$. One turn is counted if $|\Delta_w|$ exceeds 2π.

$(w > 0)$ or anticlockwise $(w < 0)$ with equal probability, and one would expect $\langle w \rangle = 0$. Hence we choose w^2 and plot $\langle w^2/L \rangle$ versus ϵ for various chain lengths in Fig. 8.

With strong adsorptive interaction, monomers of the flexible polymer are almost adsorbed. A local move parallel to the rigid polymer, from an adsorbing site to a nonadsorbing site, is energetically unfavorable. One can assume that each monomer moves only perpendicular to the rigid polymer stochastically clockwise and anticlockwise, while still keeping its distance to an adsorbing site not larger than $\sqrt{8}$, i.e., still adsorbed. Similar to $\langle \Delta_D^2 \rangle \sim t$, where Δ_D is the displacement and t is the elapsed time in one-dimensional diffusion, this assumption yields that with large ϵ

$$\langle w^2 \rangle \sim L, \tag{6a}$$

$$N_{\text{turn}} \sim L, \tag{6b}$$

where N_{turn} is the mean number of turns. For $\epsilon > 3.5$, the curves of $\langle w^2/L \rangle$ for different chain lengths collapse (see Fig. 8), which validates Eq. 6(a). We have also plotted the N_{turn} as a function of L at $\epsilon \in \{3.0,3.5,4.0,4.5,5.0\}$ in Fig. 9. The linearly fitted dashed lines for all these interaction strength confirm the above analysis too.

The flexible polymer is divided into three kinds of segments to further understand the dependence of $\langle w^2 \rangle$ on ϵ. The nonadsorbed successive monomers at the terminals of the chain are called *tail* and in the middle are called *loop*,

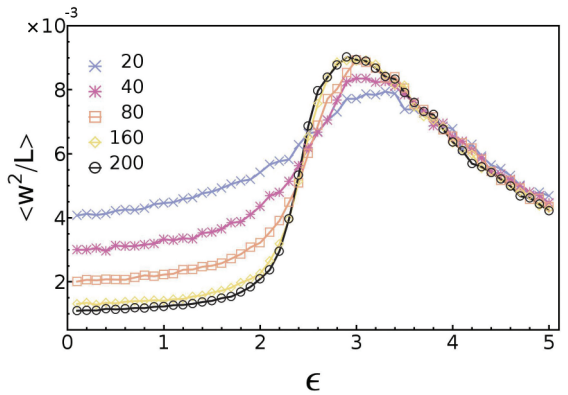

FIG. 8. (Color online) The chain length normalized mean square winding value $\langle w^2 \rangle / L$ vs the adsorption energy ϵ for different L.

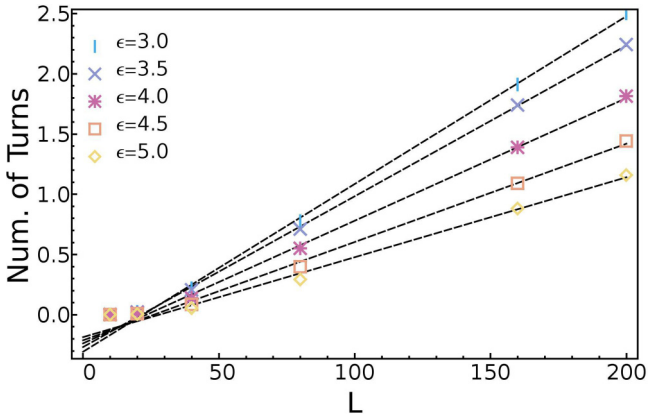

FIG. 9. (Color online) The mean number of turns N_{turn} vs the chain length L at strong adsorptive interaction $\epsilon \geqslant 3.0$. The dashed lines are the linear fitted curves.

and the adsorbed successive monomers are called *train* (see Fig. 10). Given the length of a segment L_s, we define the squared winding value per monomer for this segment as $w^2_{\text{mono}} = w^2/L_s$.

Figure 11(a) shows the fraction of monomers in tail f_{tail}, loop f_{loop}, and train f_{train} as a function of ϵ. With low attractive interaction strength, the tails dominate the polymer. With high attractive interaction strength, the majority of the monomers belong to the trains (see also Fig. 10). As ϵ increases, f_{tail} decreases and f_{train} increases monotonically. When ϵ is slightly larger than ϵ_0, since f_{tail} decreases faster than the increase of f_{train}, $f_{\text{loop}} = 1 - f_{\text{tail}} - f_{\text{train}}$ starts increasing. Hence there appears a maximum of f_{loop} in the range $2.5 < \epsilon < 3.0$, which is larger than ϵ_0. A similar relation between the adsorptive interaction strength of maximum f_{loop} and the transition point holds for adsorption of a polymer to a surface [39].

Furthermore, Fig. 11(b) presents the mean squared winding value per monomer $\langle w^2_{\text{mono}} \rangle$ versus ϵ for three kinds of segments. It shows that $\langle w^2_{\text{mono}} \rangle(\text{loop}) > \langle w^2_{\text{mono}} \rangle(\text{tail}) > \langle w^2_{\text{mono}} \rangle(\text{train})$ for $\epsilon < 4.0$. Since every monomer in a train is confined on the surface of the rigid polymer and each bond of certain length cannot step over a large $d\varphi$, $\langle w^2_{\text{mono}} \rangle(\text{train})$ is comparatively small. As for $\langle w^2_{\text{mono}} \rangle$ in the loop, compared

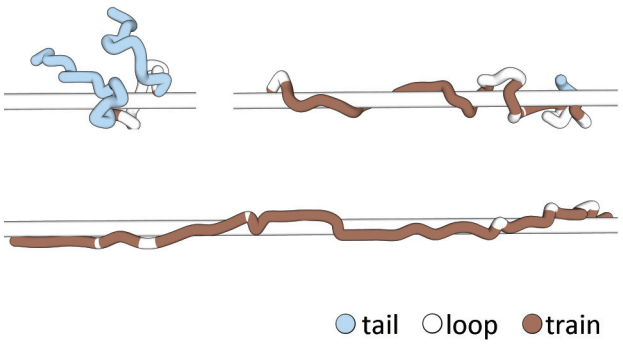

FIG. 10. (Color online) Typical conformations of a flexible polymer of chain length $L = 40$ adsorbed to a rigid polymer, with the adsorptive interaction strength $\epsilon = 0.4,2.7,4.7$ (top-left, top-right, and bottom panel, respectively). The flexible polymers are divided into three kinds of segments, tail (blue), train (brown), and loop (white).

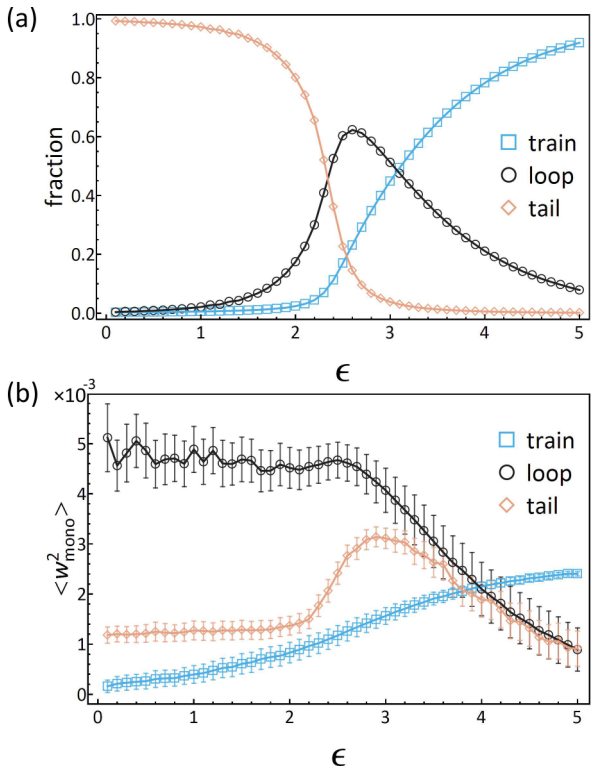

FIG. 11. (Color online) The fraction of adsorbed monomers (a) and the mean squared winding value per monomer $< w^2_{\text{mono}} >$ (b) in train, loop, and tail vs ϵ for $L = 200$.

to that in the tail, the additional grafted end impedes the nonadsorbed segment to align parallel to the rigid polymer, which hence results in a larger winding.

These two factors together explain why there is a peak for the winding of the whole chain around $\epsilon \sim 2.8$ in Fig. 8 (see also Fig. 10), where we have $\langle w^2/L \rangle \sim f_{\text{train}} \langle w^2_{\text{mono}}(\text{train}) \rangle + f_{\text{loop}} \langle w^2_{\text{mono}}(\text{loop}) \rangle + f_{\text{tail}} \langle w^2_{\text{mono}}(\text{tail}) \rangle$. Finally, we stress that the winding properties analyzed here do not necessarily mean a periodic helical conformation of the flexible polymer wrapping around the rigid one. It has been pointed out that the bending rigidity [25,26,40] and weak attraction between nonadjacent monomers of a semiflexible chain [20] play key roles in forming periodic helical winding on an adsorbing cylinder surface. We have also calculated the periodic correlation function [20] from conformations for all the studied interaction strength, and no ensemble meaningful periodicity is found.

V. CONCLUSION

In this work, we studied a generic polymer-polymer model for the adsorption of a flexible molecule onto a rigid molecule using the Monte Carlo method. In agreement with the theoretical results for the adsorption of a grafted ideal chain, our data show a steeper transition, namely, from a nonadsorbed state to an adsorbed state, in two dimensions than in three dimensions. Also considering the dependence of the Binder cumulant on the adsorption interaction strength, we conclude that there is a second-order phase transition in two dimensions and a higher-order transition in three dimensions. Both the crossing of the Binder cumulant and the ratio of the perpendicular to parallel components of the radius of gyration indicate the transition point $\epsilon \sim 2.2$ in two dimensions and $\epsilon \sim 2.1$ in three dimensions. Further analysis of the scaling of the number of adsorbed monomers with the chain length shows an expected power law relation close to the transition point. In addition, calculation of the winding value of the flexible polymer around the rigid polymer in three dimensions shows that the successive nonadsorbed monomers, which we called the *loop*, contribute most to the winding. It leads to an optimum ϵ of medium strength 2.8 for the winding of the whole chain. Here the important role played by the loop reminds us of the similar function of the linker peptide of a protein [8]. Taking the multi-C_2H_2 zinc finger protein wrapping around its target DNA site as an example, usually the C_2H_2 zinc finger domains are bound to the DNA, while the flexible linker peptides between these domains are unbound. Finally it is also shown that, with high interaction strength, the dependence of the winding and the number of turns of flexible polymer on the chain length becomes linear.

In our model, the periodicity of the adsorbing sites on the rigid polymer is set to 3, which is the integer closest to the *priori* mean bond length of a flexible polymer in the bond fluctuation model [37]. The resulting transition energy ϵ_0 is larger than that of the adsorption onto a homogeneous rigid polymer. If the periodicity is enlarged, two effects are expected. First, monomers in the flexible chain cannot be adsorbed successively any longer, and the saturation value of f_{ads} will decrease. Second, the transition energy ϵ_0 will increase. These tendencies have been investigated by other studies, such as a Monte Carlo simulation of the adsorption of periodic copolymers at a homogeneous planar substrate [41], and a numeric solution of a directed walk model of a periodic heteropolymer adsorbed onto a surface with periodic adsorbing strip pattern [42]. Changing the periodicity will shift the transition energy and the optimal winding energy, but should not change the order of the transition and the importance of loops in winding.

ACKNOWLEDGMENTS

L.L. gratefully acknowledges the funding from the Heinz Goetze Memorial Fellowship and the Heidelberg Graduate School of Mathematical and Computational Methods for the Sciences (HGS MathComp). We thank the Institute for Theoretical Physics of Heidelberg University and the high-performance cluster bwGRiD for computational resources.

[1] H. J. Dyson and P. E. Wright, Nat. Rev. Mol. Cell. Biol. **6**, 197 (2005).
[2] P. Radivojac, L. M. Iakoucheva, C. J. Oldfield, Z. Obradovic, V. N. Uversky, and A. K. Dunker, Biophysical Journal **92**, 1439 (2007).
[3] V. N. Uversky, Protein Science **11**, 739 (2002).
[4] V. N. Uversky and A. K. Dunker, Biochimica et Biophysica Acta **1804**, 1231 (2010).
[5] K. Sugase, H. J. Dyson, and P. E. Wright, Nature (London) **447**, 1021 (2007).

[6] H. Dyson, Current Opinion in Structural Biology **12**, 54 (2002).
[7] C. J. Feinauer, A. Hofmann, S. Goldt, L. Liu, G. Mt, and D. W. Heermann, in *Organisation of Chromosomes*, Advances in Protein Chemistry and Structural Biology Vol. 90, edited by R. Donev (Academic, New York, 2013), pp. 67–117.
[8] J. H. Laity, H. J. Dyson, and P. E. Wright, Journal of Molecular Biology **295**, 719 (2000).
[9] H.-X. X. Zhou and M. K. Gilson, Chem. Rev. **109**, 4092 (2009).
[10] P. L. Privalov, A. I. Dragan, C. Crane-Robinson, K. J. Breslauer, D. P. Remeta, and C. a. A. S. A. Minetti, Journal of Molecular Biology **365**, 1 (2007).
[11] D. Baskaran, J. W. Mays, and M. S. Bratcher, Chemistry of Materials **17**, 3389 (2005).
[12] R. Ramasubramaniam, J. Chen, and H. Liu, Appl. Phys. Lett. **83**, 2928 (2003).
[13] M. Numata, M. Asai, K. Kaneko, A.-H. Bae, T. Hasegawa, K. Sakurai, and S. Shinkai, J. Am. Chem. Soc. **127**, 5875 (2005).
[14] M. Naito, K. Nobusawa, H. Onouchi, M. Nakamura, K.-i. Yasui, A. Ikeda, and M. Fujiki, J. Am. Chem. Soc. **130**, 16697 (2008).
[15] X. Tu, S. Manohar, A. Jagota, and M. Zheng, Nature (London) **460**, 250 (2009).
[16] B. Gigliotti, B. Sakizzie, D. S. Bethune, R. M. Shelby, and J. N. Cha, Nano Lett. **6**, 159 (2006).
[17] A. Nish, J.-Y. Hwang, J. Doig, and R. J. Nicholas, Nature Nanotechnology **2**, 640 (2007).
[18] Y.-L. Zhao and J. F. Stoddart, Acc. Chem. Res. **42**, 1161 (2009).
[19] A. Star, E. Tu, J. Niemann, J.-C. P. Gabriel, S. C. Joiner, and C. Valcke, Proc. Nat. Acad. Sci. USA **103**, 921 (2006).
[20] I. Gurevitch and S. Srebnik, J. Chem. Phys. **128**, 144901 (2008).
[21] R. R. Johnson, A. T. C. Johnson, and M. L. Klein, Nano Lett. **8**, 69 (2008).
[22] D. Roxbury, J. Mittal, and A. Jagota, Nano Lett. **12**, 1464 (2012).
[23] L. Zandarashvili, D. Vuzman, A. Esadze, Y. Takayama, D. Sahu, Y. Levy, and J. Iwahara, Proc. Nat. Acad. Sci. USA **109**, E1724 (2012).
[24] D. Vuzman, A. Azia, and Y. Levy, Journal of Molecular Biology **396**, 674 (2010).
[25] S. S. Tallury and M. A. Pasquinelli, J. Phys. Chem. B **114**, 4122 (2010).
[26] S. S. Tallury and M. A. Pasquinelli, J. Phys. Chem. B **114**, 9349 (2010).
[27] R. J. Rubin, J. Chem. Phys. **44**, 2130 (1966).
[28] R. J. Rubin, J. Chem. Phys. **43**, 2392 (1965).
[29] A. Hanke, J. Phys.: Conden. Matter **17**, S1731 (2005).
[30] M.-b. Luo, J. Chem. Phys. **128**, 044912 (2008).
[31] E. Eisenriegler, K. Kremer, and K. Binder, J. Chem. Phys. **77**, 6296 (1982).
[32] R. Descas, J.-U. Sommer, and A. Blumen, J. Chem. Phys. **120**, 8831 (2004).
[33] R. Hegger and P. Grassberger, J. Phys. A **27**, 4069 (1994).
[34] S. Metzger, M. Mueller, K. Binder, and J. Baschnagel, J. Chem. Phys. **118**, 8489 (2003).
[35] P. G. De Gennes, Macromolecules **14**, 1637 (1981).
[36] S. Bhattacharya, V. G. Rostiashvili, A. Milchev, and T. A. Vilgis, Phys. Rev. E **79**, 030802 (2009).
[37] I. Carmesin and K. Kremer, Macromolecules **21**, 2819 (1988).
[38] K. Binder and D. W. Heermann, *The Monte Carlo Method in Statistical Physics—An Introduction* (Springer, Heidelberg, 2010).
[39] R. Roe, J. Chem. Phys. **43**, 1591 (1965).
[40] I. Kusner and S. Srebnik, Chem. Phys. Lett. **430**, 84 (2006).
[41] M. S. Moghaddam, T. Vrbová, and S. G. Whittington, J. Phys. A **33**, 4573 (2000).
[42] A. A. Polotsky, J. Phys. A **47**, 245002 (2014).